

## Projected Change in Wintertime Precipitation in California Using Projected Changes in Extratropical Cyclone Activity

LUKE OSBURN

*Monash University, Melbourne, Victoria, Australia*

KEVIN KEAY

*Bureau of Meteorology, Melbourne, Victoria, Australia*

JENNIFER L. CATTO

*College of Engineering, Mathematics and Physical Sciences, University of Exeter, Exeter, United Kingdom*

(Manuscript received 16 August 2017, in final form 31 January 2018)

### ABSTRACT

Wintertime extratropical cyclones in the east Pacific region are the source of much of the precipitation over California. There is a lot of uncertainty in future projections of Californian precipitation associated with predicted changes in the jet stream and the midlatitude storm tracks. The question this work seeks to answer is how the changes in the frequency and the intensity of extratropical cyclones in the Pacific storm track influence future changes in Californian precipitation. The authors used an objective cyclone identification method applied to 25 CMIP5 models for the historical and RCP8.5 simulations and investigated the changing relationships between storm frequency, intensity and precipitation. Cyclone data from the historical simulations and differences between the historical and RCP8.5 simulations were used to “predict” the modeled precipitation in the RCP8.5 simulations. In all models, the precipitation predicted using historical relationships gives a lower future precipitation change than the direct model output. In the future, the relationship between track density and precipitation indicates that for the same number of tracks, more precipitation is received. The relationship between track intensity and precipitation (which is quite weak in the historical simulations) does not change in the future. This suggests that other sources, likely enhanced moisture availability, are more important than changes in the intensity of cyclones for the rainfall associated with the storm tracks.

### 1. Introduction

The 2011/12 to 2013/14 three-winter average precipitation for California was the second driest that has occurred since records began in 1895 (Griffin and Anchukaitis 2014; Vose et al. 2014). In addition the average temperatures over the same time period were the highest on record (Seager et al. 2015). In January 2014 Governor Jerry Brown issued a drought state of emergency, and the total economic cost for the 2014, 2015, and 2016 drought years was 5.54 billion dollars and 31900 jobs (Howitt et al. 2014, 2015; Medellín-Azuara et al. 2016).

These three dry winter seasons were characterized by ridging in the North Pacific associated with an anomalous high pressure system off the west coast of

Washington State (Seager et al. 2015). This anomalous pattern was also associated with a northward shift of the midlatitude storm track and therefore a suppression to the west of California (Swain et al. 2014; Seager et al. 2015). Since the vast majority of California precipitation coincides with the passage of midlatitude cyclones (Cayan and Roads 1984), it is important to examine the relationship between cyclone activity in the northeast Pacific and precipitation in California, and how this may change in a projected warming climate.

Because of California’s geographic location and extent, its precipitation totals are influenced by a number of different mechanisms, each of which may be influenced by a changing climate. Such mechanisms include the displacement of the Pacific jet, subtropical dry zone, storm tracks, and the Hadley cell (Choi et al. 2016). Consequently, projected future changes for Californian

Corresponding author: Luke Osburn, lukeosburn@monash.edu

precipitation are quite uncertain (Scheff and Frierson 2012; Neelin et al. 2013; Gao et al. 2014; Maloney et al. 2014; Chang et al. 2015).

Maloney et al. (2014) examined precipitation projections using the fifth phase of the Coupled Model Intercomparison Project (CMIP5; Taylor et al. 2012) with the RCP8.5 high-emissions scenario and found that precipitation for 2070–99 relative to 1961–90 was projected to increase in Northern California and decrease in Southern California, with poor model agreement over central California. Wang and Schubert (2014) examined the effect of global warming on Californian precipitation between the periods 1871–1970 and 1980–2013 and found that there was no notable difference in the probability distribution functions of precipitation. They demonstrated that fewer storms reached California owing to an increase in positive GPH anomalies in the northern Pacific region and inferred that any decrease in storm-associated precipitation was counteracted by increases in precipitation due to increases in humidity. Swain et al. (2014) found that the extreme geopotential height values in the northeast Pacific, which are associated with California dry winters, occur more frequently in the present climate than they did in the absence of anthropogenic greenhouse gas emissions. Additionally Chang et al. (2015) found over the period 1980–2013 that there was a slight decrease in precipitation in California, but this was not statistically significant.

Chang et al. (2015) examined the role of the midlatitude storm track on the precipitation over California using the RCP8.5 scenario and identified the storm tracks using the 24-h difference filtered variance of sea level pressure (pp). They demonstrated that 1) California winter precipitation is strongly correlated to pp and 2) model-to-model differences in projected changes in California precipitation are highly correlated with model-to-model differences in projected changes in the east Pacific midlatitude storm-track activity. Additionally, they were able to predict the future precipitation changes from the RCP8.5 simulations using the historical relationships between pp and precipitation and the changes in pp between the historical and RCP8.5 simulations with a close to one-to-one relationship. Neelin et al. (2013) showed that precipitation increases in Northern California were associated with the eastward extension and strengthening of the Pacific jet stream, which steered the storm track more toward the California coast.

While future changes in the Pacific storm track will clearly have an impact on the precipitation received by California, what is currently unclear is whether these are due to changes in frequency or intensity (or other characteristics) of the extratropical cyclones. There are a number of ways of defining the storm-track activity with

pp (e.g., Chang et al. 2015) being a typical Eulerian method, which does not allow individual cyclones to be considered. Chang (2013) and Chang et al. (2015) showed a small increase in storm-track activity in the east Pacific in the RCP8.5 projections using pp as a measure of storm-track activity. Other Eulerian methods suggest a slight poleward shift of the storm tracks in this region (Chang et al. 2012; Chang 2013; Lehmann et al. 2014).

There have been fewer studies showing future projections using Lagrangian feature-tracking methods over the east Pacific region. Catto et al. (2011) showed a large increase in track density in the High-Resolution Global Environment Model (HiGEM) in an idealized quadrupled carbon dioxide experiment but a small decrease in the doubled carbon dioxide scenario. This suggests that there is even uncertainty associated with the forcings applied to the same model. Another measure related to storm-track activity is the frequency of synoptic fronts. Catto et al. (2014) showed that in the east Pacific there is an overall decrease in front frequency of around 10% of the historical values in the RCP8.5 simulations.

Changes in the intensity of extratropical tropical cyclones are also projected in a warming climate, although conflicting results for changes in intense cyclones in the Pacific (Mizuta 2012; Chang et al. 2012) have been seen that are associated with differences in the method of identifying the storm tracks (Chang 2014). A number of studies show that in a warming climate, the precipitation associated with individual extratropical cyclones is likely to increase (e.g., Watterson 2006; Champion et al. 2011; Pfahl et al. 2015), and there is a strong relationship between cyclone-related precipitation and cyclone intensity (e.g., Pfahl and Sprenger 2016). This leads to the question of how future precipitation changes in California depend on the frequency of extratropical cyclones and the intensity of those cyclones.

California receives most of its precipitation during the wintertime and the goal of the current study is to investigate the future projected changes in California wintertime precipitation, where they are the most uncertain, during the winter season comprising the consecutive months of December, January, and February (DJF). This work builds on that of Chang et al. (2015) using a Lagrangian approach rather than Eulerian, which allows both the frequency and intensity of cyclones to be used in the statistical analysis of future precipitation changes and aims to answer the following questions:

- 1) What are the relationships between cyclone track density and Californian precipitation and cyclone intensity and Californian precipitation?

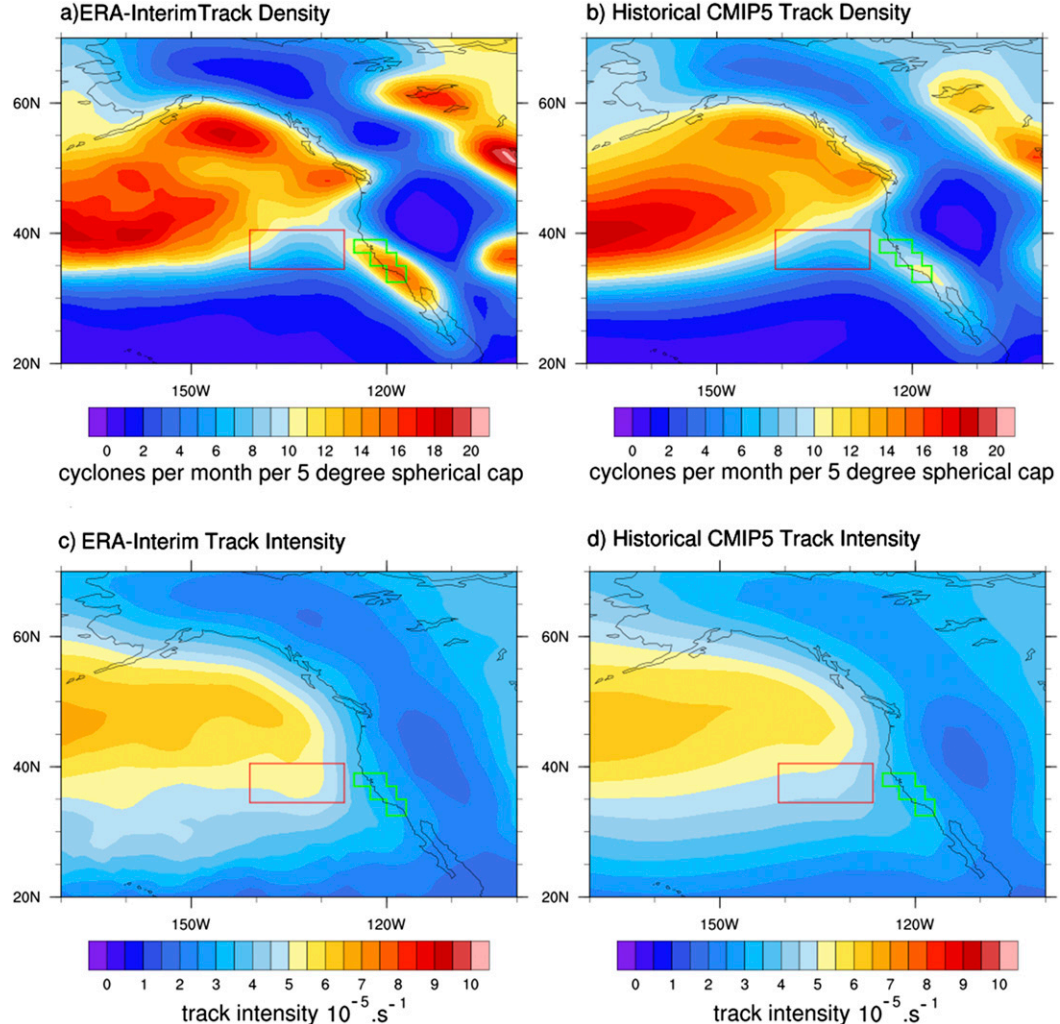


FIG. 1. Cyclone track density (cyclones per month per  $5^{\circ}$ -radius circle) from (a) ERA-Interim (1979–2005) and (b) the historical multimodel ensemble mean from the CMIP5 models (1965–2005). Cyclone track intensity from (c) ERA-Interim ( $10^{-5} \text{ s}^{-1}$ ) and the (d) historical multimodel ensemble mean of cyclone track intensity from the CMIP5 models. The boxes indicate regions used for averaging in later figures.

- 2) How are the relationships between cyclone track density and cyclone intensity and Californian precipitation projected to change in the future?
- 3) Can changes in the cyclone track density or cyclone intensity be used to predict precipitation changes in California?

The rest of the paper will be as follows. Section 2 will give a description of the observational and model data and the Lagrangian feature-tracking method. An analysis of the present-day relationship between the storm tracks and Californian precipitation will be given in section 3, and the future projections of the storm tracks and precipitation will be given in section 4.

## 2. Data and methods

### a. Data

Data from the Global Precipitation Climatology Project (GPCP; Adler et al. 2003) were used to investigate winter precipitation in California. The GPCP monthly product provides an estimated monthly rainfall on a  $2.5^{\circ}$  global grid using data from various satellite datasets and gauge data. The average precipitation within the green box shown in Fig. 1 was calculated for each winter season (DJF) from the observational data.

This box is the same as was used by both Neelin et al. (2013) and Chang et al. (2015) and was chosen because it covers the area of California where the sign of precipitation projection is uncertain.

TABLE 1. Models used in this study.

Model	Lat × lon	Model levels	Group
ACCESS1.0	1.25° × 1.85°	38	Commonwealth Scientific and Industrial Research Organization (CSIRO) and Bureau of Meteorology (BoM), Australia
ACCESS1.3	1.25° × 1.85°	38	CSIRO and BoM, Australia
BCC_CSM1.1	2.8° × 2.8°	26	Beijing Climate Center, China Meteorological Administration, China
BCC_CSM1.1(m)	2.8° × 2.8°	26	Beijing Climate Center, China Meteorological Administration, China
CanESM2	1.90° × 1.9°	35	Canadian Centre for Climate Modelling and Analysis, Canada,
CCSM4	0.9° × 1.25°	27	National Center for Atmospheric Research
CMCC-CM	0.75° × 0.75°	31	Centro Euro-Mediterraneo per I Cambiamenti Climatici, Italy
CNRM-CM5	1.4° × 1.4°	31	Centre National de Recherches Météorologiques/Centre Européen de Recherche et de Formation Avancée en Calcul Scientifique, France
CSIRO Mk3.6.0	1.9° × 1.9°	18	CSIRO in collaboration with Queensland Climate Change Centre of Excellence, Australia
FGOALS-g2	2.8125° × 2.8125°	26	LASG (Institute of Atmospheric Physics), Tsinghua University, China
GFDL-ESM2G	2.0° × 2.5°	24	NOAA/Geophysical Fluid Dynamics Laboratory
GFDL-ESM2M	2.0° × 2.5°	24	NOAA/Geophysical Fluid Dynamics Laboratory
HadGEM2-CC	1.2° × 1.9°	60	Met Office Hadley Centre, United Kingdom
HadGEM2-ES	1.2° × 1.9°	38	Met Office Hadley Centre, United Kingdom
INM-CM4.0	2.0° × 1.5°	21	Institute of Numerical Mathematics, Russia
IPSL-CM5A-LR	1.90° × 3.75°	39	L'Institut Pierre-Simon Laplace, France
IPSL-CM5A-MR	1.25° × 2.50°	39	L'Institut Pierre-Simon Laplace, France
IPSL-CM5B-LR	1.90° × 3.75°	39	L'Institut Pierre-Simon Laplace, France
MIROC5	1.4° × 1.4°	40	Atmosphere and Ocean Research Institute (The University of Tokyo), National Institute for Environmental Studies, and Japan Agency for Marine-Earth Science and Technology, Japan
MIROC-ESM	2.8° × 2.8°	80	Atmosphere and Ocean Research Institute (The University of Tokyo), National Institute for Environmental Studies, and Japan Agency for Marine-Earth Science and Technology, Japan
MIROC-ESM-CHEM	2.8° × 2.8°	80	Atmosphere and Ocean Research Institute (The University of Tokyo), National Institute for Environmental Studies, and Japan Agency for Marine-Earth Science and Technology, Japan
MPI-ESM-LR	1.9° × 1.9°	47	Max Planck Institute for Meteorology, Germany
MPI-ESM-MR	1.9° × 1.9°	95	Max Planck Institute for Meteorology, Germany
MRI-CGCM3	1.125° × 1.125°	48	Meteorological Research Institute, Japan
NorESM1-M	1.9° × 2.5°	26	Norwegian Climate Centre, Norway

The data used to calculate the storm-track statistics were taken from the European Centre for Medium-Range Weather Forecasts (ECMWF) interim reanalysis (ERA-Interim; [Dee et al. 2011](#)). Six-hourly winds (zonal and meridional;  $u$  and  $v$ ) at 850 hPa from DJF 1979/80 to 2009/10 were used to calculate the vorticity required for the tracking algorithm (described below). The data were extracted at 1.5° resolution.

Data from 25 CMIP5 models ([Taylor et al. 2012](#)) from 16 different modeling centers were used in the model analysis, and these are shown in [Table 1](#). Present-day data were taken from the historical simulations for the 40 DJF seasons from the years 1965/66 to 2004/05. Future climate scenario data were taken from the RCP8.5 scenario simulations for the 40 DJF seasons from the years 2060/61 to 2099/2100, except for BCC\_CSM1.1, BCC\_CSM1.1(m), and HadGEM2-ES, for which the 40 DJF seasons were from the years 2059/60–98/99 and

for CMCC-CM, for which data were only available between 2080/81 and 2099/2100. For the extratropical cyclone identification the 6-hourly fields were used, and for the precipitation analysis, the monthly values were added together to make the seasonal total. The RCP8.5 scenario was used in order to provide a strong signal, consistent with the methodologies of [Neelin et al. \(2013\)](#) and [Chang et al. \(2015\)](#). The r1i1p1 initializations for the CMIP5 models were used with the exception of CCSM4 for which the r6i1p1 initialization was used. The required data (6-hourly  $u$  and  $v$  and monthly precipitation) were extracted on each model's native resolution. The average precipitation in the California region was calculated by using the area-weighted average precipitation from grid cells within the green box shown in [Fig. 1](#).

All linear regressions were tested for statistical significance at the 5% confidence level and (with the

exceptions of Figs. 3c and 7b shown below) were found to be statistically significant.

### b. Extratropical cyclone identification and tracking

Extratropical cyclones are identified with the method of Hodges (Hodges 1994, 1995). Features are identified as maxima (in the Northern Hemisphere) of 850-hPa vorticity, which is first truncated to T42 resolution (approximately 300-km grid spacing) to focus on the synoptic scales. The feature points, found at each 6-hourly time point, are initially linked using a nearest-neighbor approach, and then the “best” tracks are found by minimizing a cost function based on the smoothness of the ensemble of tracks.

A major advantage of using a Lagrangian objective feature identification and tracking algorithm is that information about the number or frequency of tracks, as well as their intensity, can be obtained. This is in contrast to the Eulerian method of identifying the storm tracks using measures of the variance of mean sea level pressure (Chang et al. 2015), geopotential height, or eddy kinetic energy.

Track density and track intensity obtained from the feature tracking are used in this study. Track density is a measure of the number of tracks passing through a region and is calculated as a number of cyclones per unit time per unit area (cyclones per month per  $5^\circ$  radius circle). Track intensity is a measure of the T42 resolution vorticity of the cyclones and is calculated using all points along the track, so that if a cyclone is slow moving, it may contribute more to the average intensity at a grid point than a fast-moving cyclone (shown in units of  $10^{-5} \text{ s}^{-1}$ ).

## 3. Historical period

### a. Extratropical cyclone tracking statistics

First the track density and track intensity from ERA-Interim and the CMIP5 models are analyzed. Figure 1 shows these metrics for ERA-Interim and the multimodel mean for the historical simulation. The track density from ERA-Interim shows a region of high values over the east Pacific Ocean, with a maximum of about 18 cyclones per month around  $40^\circ\text{N}$  and close to the coast around  $55^\circ$  and  $50^\circ\text{N}$ . There is a smaller local maximum farther south just over the coast of Southern California. There is a large region over the Rocky Mountains where the track density is very low. There is good agreement in quantity of track density over the North Pacific; however, the CMIP5 models do produce lower track density values over California and south of Alaska. The track intensity from ERA-Interim shows a maximum between  $45^\circ$  and  $50^\circ\text{N}$ , which is generally well represented by the CMIP5 models.

Chang et al. (2015) used pp from the National Centers for Environmental Prediction reanalysis (Kalnay et al. 1996) as a measure for the storm track shown in Fig. 1 of Chang et al. (2015), and it is generally spatially consistent with the track density produced by the ERA-Interim reanalysis; however, it does not show the local maxima in track density that occur over California and south of Alaska. It also does not show such a distinct minimum over the Rockies, since here the MSLP will vary even though individual storms would not continue over the high orography.

### b. Relationship between extratropical cyclones and precipitation

Maps of the temporal correlation between average seasonal GPCP precipitation in the California box and track density from ERA-Interim and between GPCP precipitation and track intensity are shown in Figs. 2a,c. Considering the correlation between track density and Californian precipitation, there is a large region of positive correlation in the eastern Pacific with the highest values (of about 0.8) just to the west of California. The correlation pattern between Californian precipitation and track intensity is more spatially spread out with high values in a number of places over the east Pacific. The correlation between track density and Californian precipitation has a similar spatial pattern to the correlation between precipitation and pp shown in Chang et al. (2015), although the maximum correlation is farther north for the track density.

The same correlations, averaged over the CMIP5 multimodel ensemble (MME), are shown in Figs. 2b,d. The correlation between the CMIP5 MME means of track density and modeled precipitation shows a maximum in the same location as the observations (Fig. 2a) and is generally spatially consistent with a maximum of about 0.5. The CMIP5 correlation between track intensity and precipitation shows a spatial pattern that is much more coherent than the observations and has a maximum of about 0.4 to the west of California. Averaging over 25 CMIP5 models does smooth the results for the MME; however, individual models do produce results comparable to the observations.

A linear regression between Californian precipitation and the tracking statistics is calculated using the average tracking statistics in the red box shown in Fig. 2, which is between  $34.5^\circ$  and  $40.5^\circ\text{N}$  and  $126.5^\circ$  and  $141^\circ\text{W}$ . This box was chosen as it generally captures the areas of highest correlation between track density and precipitation and between track intensity and precipitation over California from the reanalysis data as well as from the CMIP5 models. This study was repeated with a much larger box ranging from  $35^\circ\text{S}$  to  $49^\circ\text{N}$  and from  $125^\circ$  to  $138^\circ\text{W}$  in order to determine the sensitivity of our results

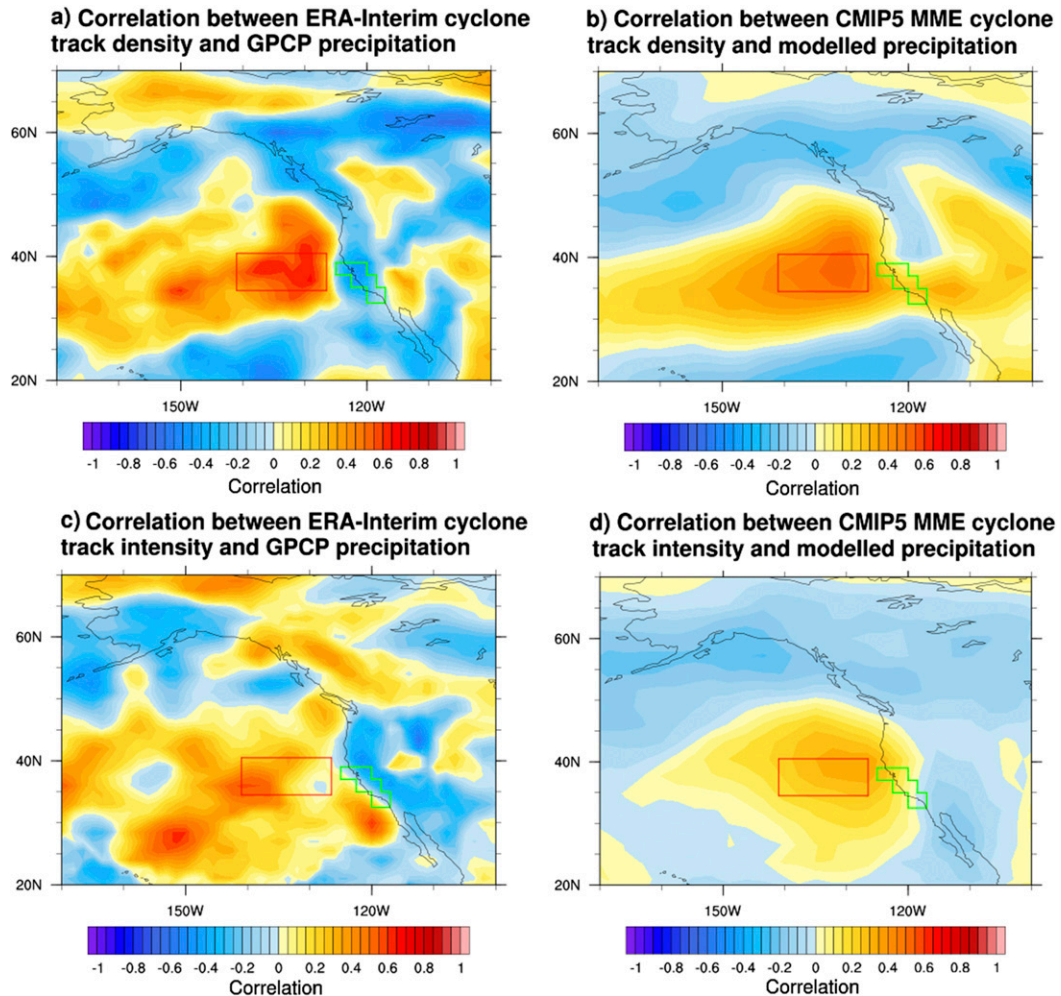


FIG. 2. Correlation between (a) DJF cyclone track density (cyclones per month per  $5^{\circ}$ -radius circle) from ERA-Interim and the average DJF GPCP precipitation within the green box from 1979–2005 and the (b) correlation between DJF cyclone track density from the CMIP5 models and the DJF modeled precipitation within the green box from 1965–2005. Correlation between (c) DJF cyclone track intensity from ERA-Interim and the average DJF GPCP precipitation within the green box from 1979–2005 and (d) the correlation between DJF cyclone track intensity ( $10^{-5} \text{ s}^{-1}$ ) from the CMIP5 models and the modeled DJF precipitation within the green box from 1965–2005. The boxes indicate regions used for averaging in later figures.

to box size and location. Overall, the results are similar, and the conclusions of this study are unaffected.

The historical relationship between Californian precipitation and cyclone track density from the reanalysis and observational precipitation record is shown in Fig. 3a. The correlation between Californian precipitation and east Pacific track density is high at 0.71, and the linear regression between the two variables gives a slope of  $0.40 \text{ mm day}^{-1}$  per unit track density. The same relationship for the CMIP5 models is shown in Fig. 3b. Each year from each CMIP5 model is plotted, producing 1000 data points. Using all the data in this way gives a correlation from the CMIP5 models of 0.68, and the same slope is found for the linear regression ( $0.40 \text{ mm day}^{-1}$  per unit

track density). The historical correlations and slopes between precipitation and track density for the individual models are shown in Table 2. The spread of correlation values between track density and precipitation varies from 0.29 for GFDL-ESM2G to 0.87 for CCSM4, with 13 models having correlation values greater than 0.65. GFDL-ESM2G does produce an area of high correlation between track density and precipitation but it is located at  $48^{\circ}\text{N}$  (not shown). There is generally good agreement regarding the relationship between track density and precipitation with 12 models producing slopes between 0.35 and  $0.50 \text{ mm day}^{-1}$  per unit track density.

The relationship between precipitation and east Pacific averaged track intensity for the observations is

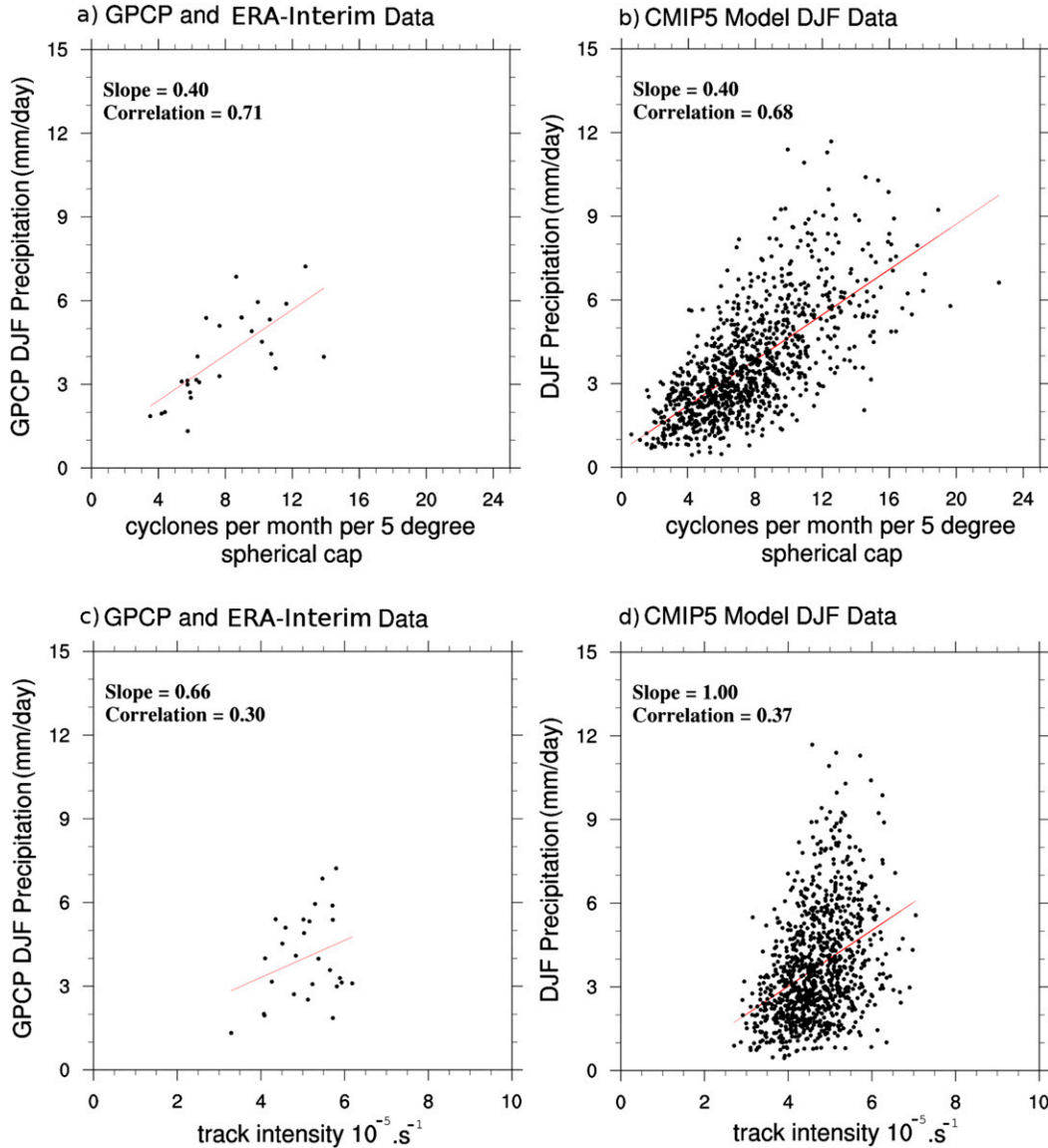


FIG. 3. Historical relationship from (a) observed DJF data (1979–2005) of precipitation over California to the DJF cyclone track density (cyclones per month per  $5^{\circ}$ -radius circle) from ERA-Interim and the relationship of the same variables from the (b) CMIP5 models (1965–2005). Historical relationship from (c) observed data of precipitation over California to the track intensity ( $10^{-5} \text{ s}^{-1}$ ) from ERA-Interim and the relationship of the same variables from the (d) CMIP5 models.

shown in Fig. 3c and gives a much lower correlation of 0.3. Over all the models (Fig. 3d) the correlation is 0.37, which is close to the observed value. The historical correlations and slopes of the linear regressions between precipitation and track intensity for the individual models are also shown in Table 2. There is a greater difference between the models in the relationships between track intensity and precipitation compared to those for track density. Correlations vary from -0.10 to 0.75 with 18 models producing correlation values

between 0.2 to 0.5. There is also a wide range in the values of the slopes of the linear regressions between track intensity and precipitation ranging from -0.34 to  $1.86 \text{ mm day}^{-1} 10^5 \text{ s}$ , with 10 models producing values between 0.75 to  $1.25 \text{ mm day}^{-1} 10^5 \text{ s}$ .

A comparison of these results with those from Chang et al. (2015) show that the MME correlation between Californian precipitation and track density (Fig. 2b) is spatially consistent with that for pp, although the correlations using track density are lower.

TABLE 2. Historical correlations and slopes for the individual models. Models are statistically significant if the correlation is greater than 0.31.

Model	Track density slope	Track density correlation	Track intensity slope	Track intensity correlation
ACCESS1.0	0.47	0.67	1.29	0.47
ACCESS1.3	0.52	0.74	0.50	0.20
BCC_CSM1.1	0.18	0.52	0.76	0.49
BCC_CSM1.1(m)	0.29	0.49	0.79	0.27
CanESM2	0.27	0.69	0.64	0.38
CCSM4	0.40	0.87	1.86	0.75
CMCC-CM	0.33	0.49	0.64	0.20
CNRM-CM5	0.17	0.44	0.29	0.18
CSIRO Mk3.6.0	0.34	0.66	-0.34	-0.10
FGOALS-g2	0.19	0.53	1.15	0.47
GFDL-ESM2G	0.14	0.29	0.39	0.26
GFDL-ESM2M	0.25	0.66	1.12	0.48
HadGEM2-CC	0.42	0.77	1.13	0.38
HadGEM2-ES	0.40	0.74	0.92	0.48
INM-CM4.0	0.37	0.56	1.26	0.53
IPSL-CM5A-LR	0.41	0.59	0.76	0.27
IPSL-CM5A-MR	0.41	0.71	1.57	0.55
IPSL-CM5B-LR	0.32	0.39	1.49	0.32
MIROC5	0.44	0.80	0.96	0.36
MIROC-ESM	0.28	0.68	0.27	0.21
MIROC-ESM-CHEM	0.19	0.48	0.26	0.26
MPI-ESM-LR	0.48	0.76	0.28	0.12
MPI-ESM-MR	0.46	0.64	1.14	0.47
MRI-CGCM3	0.46	0.58	1.67	0.40
NorESM1-M	0.42	0.77	0.85	0.44

#### 4. Future projections

##### a. Extratropical cyclone tracking statistics

Future projections are based on using the RCP8.5 scenario from the CMIP5 models for the period 2060/61–2099/2100 (except where detailed in section 2a). Changes in the storm tracks using the measures of track density and track intensity are shown in Fig. 4. The black contours denote the number of models that agree with a positive change while the red contours denote the number of models that agree with a negative change. There is generally good agreement with between 15 and 20 models projecting an increase in track density south of 60°N down to 35°N off the U.S. West Coast (Fig. 4a). The MME mean of variance of track density within the red box increases from 7.37 to 7.82 (cyclones per month per 5°-radius circle)<sup>2</sup> between the historic and RCP8.5 simulations with 14 models projecting an increase.

This pattern represents a poleward shift in the mid-latitude storm track over the North Pacific and is consistent with the recent work of Tamarin-Bordsky and Kaspi (2017) and a number of other measures of storm-track activity, such as eddy kinetic energy (e.g., Lehmann et al. 2014), but is somewhat different to the measure pp used by Chang et al. (2015). For pp there is a

local increase off the U.S. West Coast at 40°N, but no clear shift. Between 150°W and the American coastline the track density increases and extends equatorward with a maximum in the shift occurring at 47°N.

There is good agreement on a negative change in track intensity south of 40°N and a positive change north of 50°N (Fig. 4b). However, the gradient of positive to a negative change of track intensity is not as sharp as it is for track density. There is a small decrease in the MME of track intensity in the domain of interest, although an increase at 48°N does occur.

##### b. Relationship between extratropical cyclones and precipitation

Maps of the temporal correlations of track density and track intensity with California precipitation from the RCP8.5 scenario are shown in Fig. 5. There is a general increase in the correlation between track density and precipitation between 30° and 45°N and the size of the area that has a positive correlation over the North Pacific is larger than in the historical simulations. Comparing with Fig. 2b, the extent of positive temporal correlations of track intensity with precipitation extends westward at 40°N and poleward at 150°W, although the correlations off the U.S. West Coast remain relatively unchanged (compared with Fig. 2d).

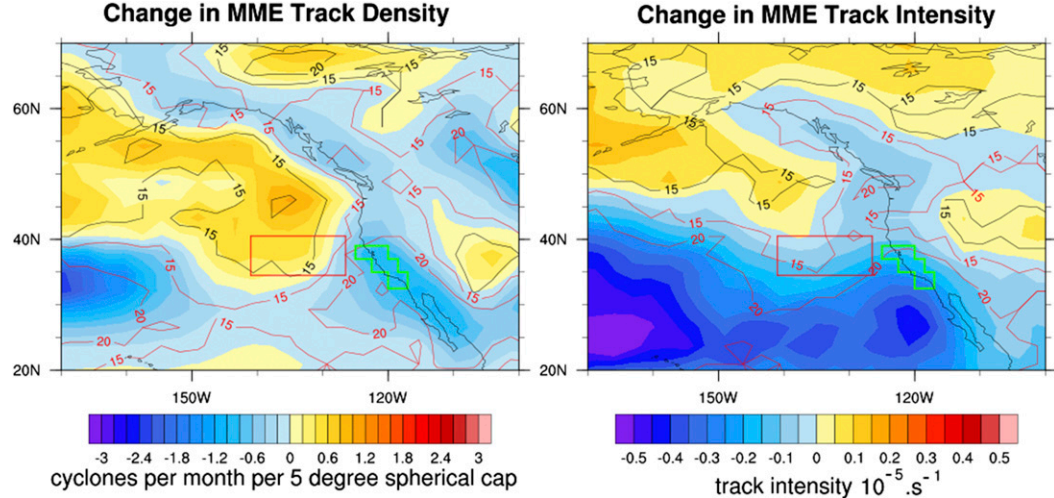


FIG. 4. Change in the multimodel ensemble mean of (a) cyclone track density (cyclones per month per  $5^{\circ}$ -radius circle) and (b) track intensity ( $10^{-5} \text{ s}^{-1}$ ) between the RCP8.5 (2060–2100) and historical simulations (1965–2005). The black contours denote the number of models that agree with a positive change while the red contours denote the number of models that agree with a negative change.

The relationships between DJF precipitation and east Pacific averaged cyclone track density and intensity from the RCP8.5 simulations are shown in Fig. 6. The slope of the linear regression and correlation between cyclone track density and precipitation in California both increase under the RCP8.5 scenario from 0.40 to 0.50  $\text{mm day}^{-1}$  per unit track density and from 0.68 to 0.76, respectively. There is good model agreement regarding the direction of these changes with 19 models projecting an increase in the slope of the linear regression between cyclone track density and precipitation and with 17 models projecting

an increase in the correlation. These results suggest that for the same number of cyclone tracks, the precipitation is projected to increase.

The slope of the linear regression between track intensity and precipitation in California increases from 1.00 in the historical simulations to  $1.36 \text{ mm day}^{-1} 10^5 \text{ s}$  in the RCP8.5 scenario and the correlation increases from 0.37 to 0.39. There is good model agreement regarding the increase in the slope of the linear regression between track intensity and precipitation with 19 models projecting an increase while only 14 models project an

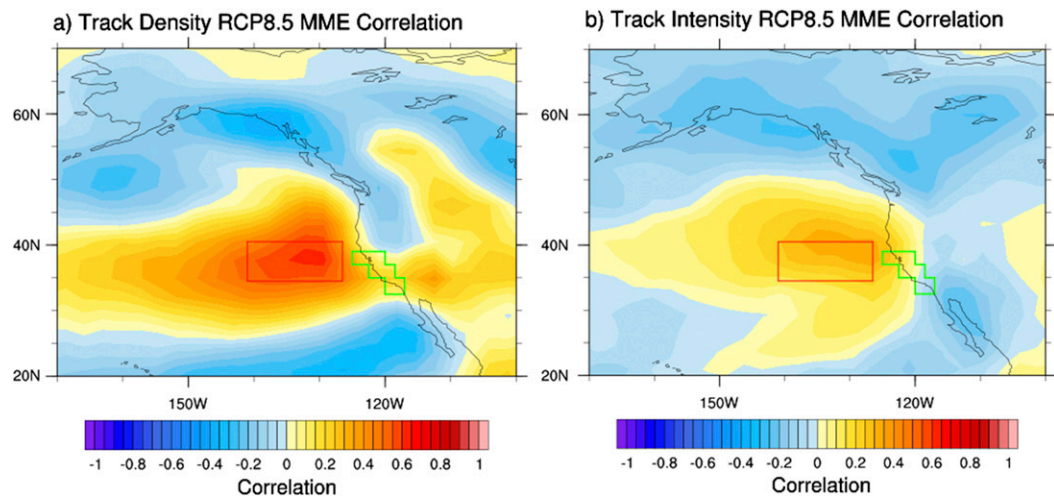


FIG. 5. Multimodel ensemble mean of the correlations between (a) DJF cyclone track density (cyclones per month per  $5^{\circ}$  radius circle) from the CMIP5 RCP8.5 scenario (2060–2100) to the modeled DJF precipitation over California and the same for (b) track intensity ( $10^{-5} \text{ s}^{-1}$ ). The boxes indicate regions used for averaging in later figures.

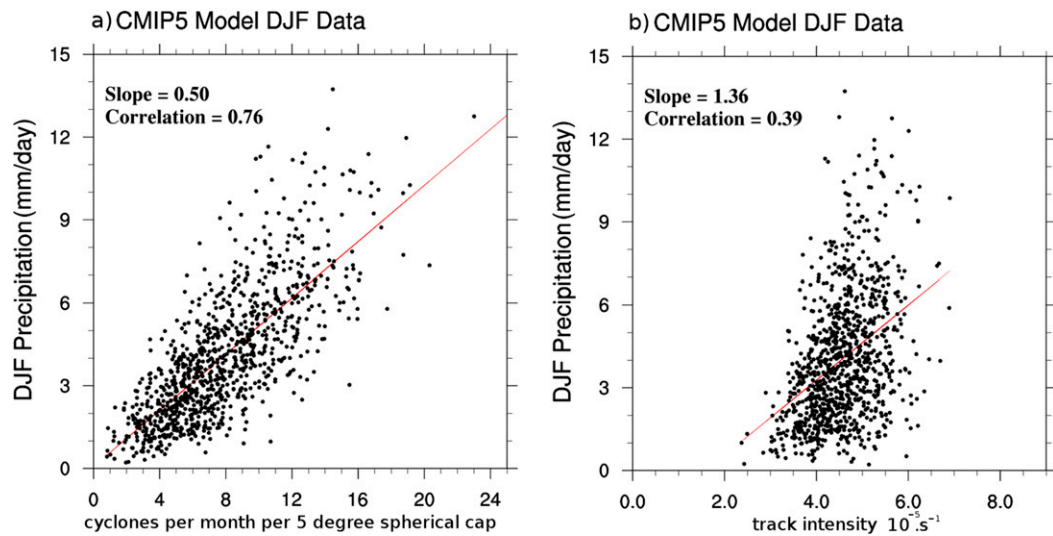


FIG. 6. Relationship between (a) DJF cyclone track density (cyclones per month per  $5^{\circ}$ -radius circle) from the CMIP5 RCP8.5 scenario (2060–2100) and the DJF precipitation over California and (b) the relationship between track intensity ( $10^{-5} \text{ s}^{-1}$ ) and precipitation.

increase in correlation. This changing relationship shows that for the same cyclone intensity, the precipitation will increase. These changes in the relationships between cyclone track density and track intensity and precipitation suggest that within the RCP8.5 scenario, if the number and strength of cyclones stayed the same, the precipitation would still increase.

The performance of the individual models in the RCP8.5 scenario for correlation and the slope of the linear regression between California precipitation and track density and track intensity are shown in Table 3. All the models produce a correlation value between track density and precipitation of greater than or equal to 0.5 with 16 models producing a correlation value greater than or equal to 0.7. The relationship between track density and precipitation is fairly consistent with 21 models producing a slope between 0.3 to 0.6  $\text{mm day}^{-1}$  per unit track density.

Similar to the historical simulations there is a greater range of correlation and slope of linear regression between precipitation and track intensity compared to track density. Correlation values varied between 0.11 to 0.64 with 17 models producing correlations between 0.2 and 0.5. The slope of the linear regression between track intensity and precipitation varies between 0.32 and  $3.14 \text{ mm day}^{-1} 10^5 \text{ s}$  with 12 models producing a slope between 0.75 and  $1.5 \text{ mm day}^{-1} 10^5 \text{ s}$ .

### c. Precipitation projections

There is poor model agreement regarding the precipitation changes in California within the RCP8.5

scenario, which can be seen in Fig. 7 and was shown in previous studies (Maloney et al. 2014). The multimodel ensemble mean projects an increase of  $0.41 \text{ mm day}^{-1}$  when comparing the two periods; however, there is a large divergence between the individual models. MIROC-ESM projects a decrease of  $-0.81 \text{ mm day}^{-1}$  while MRI-CGCM3 projects an increase of  $2.12 \text{ mm day}^{-1}$ . Data for the CMCC-CM model for the RCP8.5 scenario was only available from 2080–2100 and is therefore excluded for the precipitation projection calculations. Of the 24 models used within this analysis, 16 project a precipitation increase while 8 project a decrease.

Chang et al. (2015) found that the CMIP5 precipitation projections could be predicted by using changes in pp between the historical and the RCP8.5 simulations. In this study we attempted to use the changes in cyclone track density and cyclone intensity between the historical and RCP8.5 simulations to predict the change in precipitation between the historical and the RCP8.5 simulations.

Precipitation change in California was “predicted” with the same methodology used by Chang et al. (2015) in the following way. For each model the slope of the linear regression between cyclone track density and Californian precipitation in the historical simulations was multiplied by the change in track density between the RCP8.5 and historical simulations. This “predicted precipitation change” was compared to the precipitation change between the historical and the RCP8.5 simulations. The results are shown in Figs. 7a and 7b for changes in track density and track intensity, respectively. The

TABLE 3. RCP8.5 correlations and slopes for the individual models. Models are statistically significant if the correlation is greater than 0.31.

Model	Track density slope	Track density correlation	Track intensity slope	Track intensity correlation
ACCESS1.0	0.38	0.63	0.69	0.23
ACCESS1.3	0.50	0.58	0.88	0.17
BCC_CSM1.1	0.32	0.65	0.89	0.44
BCC_CSM1.1(m)	0.51	0.74	1.95	0.53
CanESM2	0.54	0.86	1.74	0.47
CCSM4	0.53	0.81	0.99	0.33
CMCC-CM	0.62	0.76	2.27	0.60
CNRM-CM5	0.42	0.66	0.77	0.20
CSIRO Mk3.6.0	0.36	0.73	0.84	0.26
FGOALS-g2	0.29	0.53	1.71	0.55
GFDL-ESM2G	0.49	0.70	0.89	0.33
GFDL-ESM2M	0.43	0.77	0.94	0.35
HadGEM2-CC	0.49	0.81	1.14	0.41
HadGEM2-ES	0.40	0.67	1.08	0.38
INM-CM4.0	0.46	0.83	1.69	0.51
IPSL-CM5A-LR	0.69	0.77	1.58	0.48
IPSL-CM5A-MR	0.59	0.71	3.14	0.64
IPSL-CM5B-LR	0.54	0.61	1.29	0.20
MIROC5	0.52	0.85	1.51	0.47
MIROC-ESM	0.16	0.50	0.42	0.44
MIROC-ESM-CHEM	0.38	0.76	0.32	0.24
MPI-ESM-LR	0.56	0.71	0.68	0.20
MPI-ESM-MR	0.51	0.80	1.37	0.45
MRI-CGCM3	0.38	0.64	0.51	0.11
NorESM1-M	0.32	0.73	0.79	0.47

assumptions are that the precipitation changes in California can be predicted using only changes in the mid-latitude cyclones over the North Pacific and that the relationship between midlatitude cyclones and precipitation is constant.

The utilization of track density within this methodology underestimates the projected precipitation changes from the models. As shown in Fig. 7a this relationship is characterized by the slope of the linear regression of  $1.72 \text{ mm day}^{-1}$  per unit track density. The predicted precipitation change is less than the change between the historical and RCP8.5 simulations but with a high correlation of 0.88. A slope of  $1 \text{ mm day}^{-1}$  per unit track density would indicate a perfect prediction. The root-mean-squared error (RMSE) and the y intercept of the linear regression are also shown. Change in track density is an important predictor for precipitation changes, but it is insufficient when used in isolation.

Utilizing track intensity to predict the precipitation change results in a linear regression with a slope of  $1.10 \text{ mm day}^{-1} 10^5 \text{ s}$  between the precipitation change and the predicted precipitation change. However, when compared to the utilization of track density to predict the precipitation change, the correlation decreases to 0.29, the RMSE more than doubles to  $0.67 \text{ mm day}^{-1}$ , and the y intercept increases to 0.47, indicating that

track intensity on its own is not a good predictor for precipitation change.

The incorporation of track density and track intensity in a multivariate approach is shown in Fig. 8. The correlation decreases from 0.88 to 0.82, the RMSE increases from 0.33 to  $0.39 \text{ mm day}^{-1}$ , and the y intercept increases from 0.17 to 0.27. The slope of the linear regression does reduce from 1.72 to 1.51; however, all the other evaluation metrics worsen. This indicates that the multivariate approach gives a model that does not fit the data as well and still does not account for the large differences between the statistical predictions and the precipitation change in the models.

#### d. Predictions for the historic and RCP8.5 time period

The utilization of the track density changes between the RCP8.5 and the historical simulations and the slope of the historical linear regressions between track density and precipitation to predict the precipitation projections from the CMIP5 models resulted in a substantial underestimate of projected rainfall (Fig. 7a). This prediction methodology was repeated over two shorter time periods in order to better understand this result. The first halves of the historical and RCP8.5 simulations were used to predict the precipitation of the second halves using the same methodology. For example, the slope of

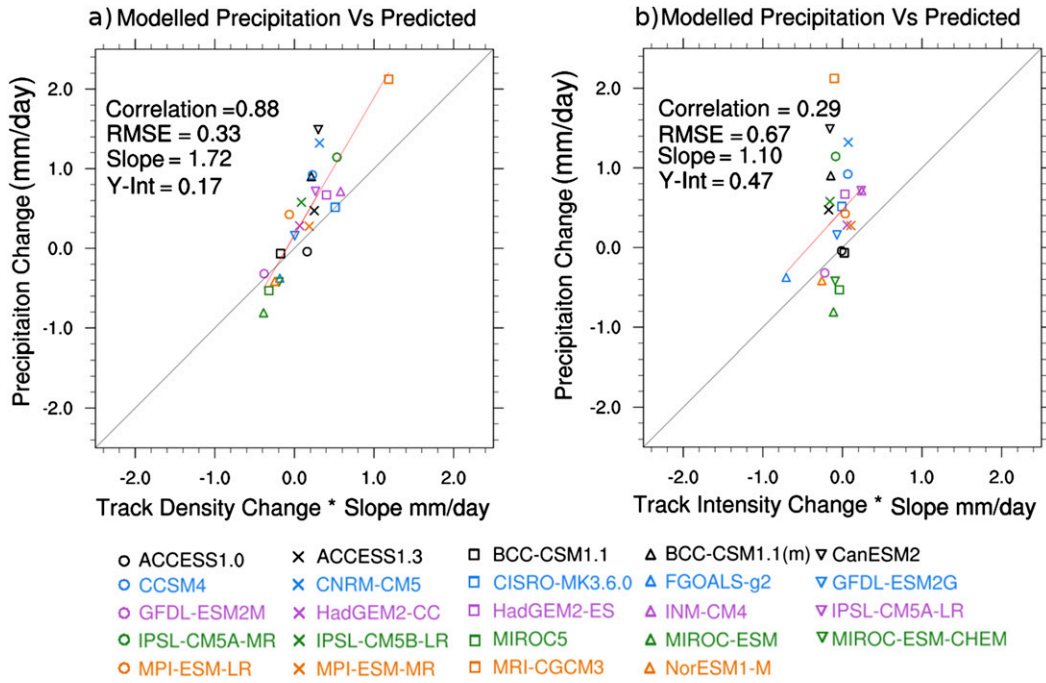


FIG. 7. Predicted precipitation based on the (a) DJF track density (cyclones per month per  $5^{\circ}$ -radius circle) change between the RCP8.5 scenario (2059–60) and the historical simulations (1965–2005) multiplied by the historical relationship between track density and precipitation for each model individually and (b) the identical procedure for track intensity ( $10^{-5} \text{ s}^{-1}$ ). Individual models are uniquely identified by a shape and color. Precipitation change for individual models is shown on the y axis, while predicted precipitation is shown on the x axis. The linear regression is shown in red while the line  $y = x$  is shown in gray.

the linear regression of Californian precipitation with east Pacific cyclone track density between 1965 and 1985 was multiplied by the cyclone track density change between 1965–85 and 1985–2005 to predict the precipitation change between these two time periods and is shown in Fig. 9a. This method was repeated for the RCP8.5 scenario from 2060 to 2100, and the results are shown in Fig. 9b. This analysis was only performed for track density owing to the stronger relationship between track density and precipitation.

The correlation of the linear regression for the historical period is 0.51, with an RMSE of  $0.39 \text{ mm day}^{-1}$ ,  $y$  intercept of 0.06, and slope of  $0.94 \text{ mm day}^{-1}$  per unit track density, and is shown in red in Fig. 9a. The correlation of the linear regression for the RCP8.5 scenario is 0.79, with an RMSE of  $0.43 \text{ mm day}^{-1}$ ,  $y$  intercept of 0.24, slope of  $1.23 \text{ mm day}^{-1}$  per unit track density, and is shown in red in Fig. 9b. The properties of extratropical cyclones within global climate models can depend on their resolution (Champion et al. 2011), and the slopes and correlations were recalculated with the lower-resolution models (gridbox area greater than  $6^{\circ}$  squared) were excluded and are shown in black. The excluded models are indicated with a red circle in

Figs. 9a,b. The precipitation predictions for the historical period are improved by excluding the low-resolution models and the correlation increases from 0.51 to 0.65, the RMSE reduces from 0.39 to  $0.32 \text{ mm day}^{-1}$ , the slope increases from 0.94 to  $1.01 \text{ mm day}^{-1}$  per unit track density, and the  $y$  intercept improves from 0.06 to  $-0.02$ . These results indicate that precipitation changes during the historical period can be predicted using only changes in cyclone track density.

Predicting precipitation for the RCP8.5 scenario future period is sensitive to the time periods used (i.e., using 36 or 38 of the DJF seasons instead of the full 40 available, shown in Fig. 9b). Additionally, excluding the low-resolution models does not consistently improve the correlation between the precipitation change and the predicted precipitation. However, the correlations are consistently high—commonly greater than 0.9—and the slopes of the linear regressions are typically between 1.2 and  $1.4 \text{ mm day}^{-1}$  per unit track density.

## 5. Discussion and conclusions

Precipitation in California is strongly driven by mid-latitude cyclones in the east Pacific during DJF. Swain

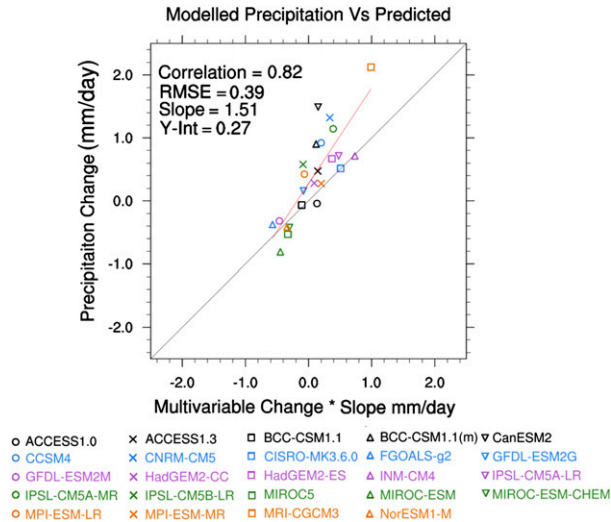


FIG. 8. Relationship between predicted precipitation using a multivariable correlation approach using track density and track intensity between the RCP8.5 scenario (2059–60) and the historical simulations (1965–2005) and the modeled precipitation change. Individual models are uniquely identified by a shape and color. The linear regression is shown in red while the line  $y = x$  is shown in gray.

et al. (2014) concluded that, owing to anthropogenic influences, the likelihood of extreme high pressure anomalies occurring off the west coast of North America increases. These high pressure anomalies are associated with the driest 15% of Californian winters, obstructing the passage of midlatitude cyclones (Seager et al. 2015). Following on from the work of Chang et al. (2015) we used a Lagrangian feature-tracking method to study the changing relationships between extratropical cyclone frequency and intensity and Californian precipitation due to climate change. This provides a complementary approach to previous studies using Eulerian storm-track measures.

East Pacific winter storm-track density and California precipitation are strongly correlated during both the historical period and the RCP8.5 scenario, and the slope of the linear regression increases from  $0.4 \text{ mm day}^{-1}$  per unit track density during the historical period to  $0.5 \text{ mm day}^{-1}$  per unit track density in RCP8.5. The correlations relating Californian precipitation to cyclone intensity for the historical period and the future period in the RCP8.5 scenario are weak at 0.37 and 0.39, respectively. The slope of the linear regression between Californian precipitation and east Pacific cyclone intensity for the historical period is  $1.00 \text{ mm day}^{-1} 10^5 \text{ s}$  and increases to  $1.36 \text{ mm day}^{-1} 10^5 \text{ s}$  in the future scenario. Changes in the spatial patterns of track density and track intensity are consistent with previous studies (e.g., Tamarin-Bordsky and Kaspi 2017), showing a

poleward shift in the track density and intensity. However, these patterns are slightly different to the pattern seen using 24-h filtered variance of mean sea level pressure (pp) as used in Chang et al. (2015). The shifts result in an overall increase in track density and very slight decrease in track intensity in the east Pacific box used in this study.

Following the methodology of Chang et al. (2015), these historical relationships and future changes in tracking statistics were then used to predict the precipitation projections over California in the RCP8.5 scenario resulting in underestimated precipitation changes from future projections in the CMIP5 models. Indeed, the linear regressions between precipitation and track density and between precipitation and track intensity in the future have steeper slopes than in the historical period, indicating more precipitation for the same number and strength of cyclones. We did, however, find that it is possible to predict the CMIP5 precipitation projections when the first half of the historical period is used to predict the second half (Fig. 9a). This is a robust result, with an RMSE of  $0.32 \text{ mm day}^{-1}$ , correlation of 0.65, slope of  $1.01 \text{ mm day}^{-1}$  per unit track density, and a y intercept of  $-0.02$ . However, this methodology does not work for the RCP8.5 scenario (Fig. 9b), and the results for the RCP8.5 scenario are sensitive to the time periods used. This additional analysis suggests that over the historical period, the relationship between extratropical cyclones and precipitation does not change much, but even over the 40 years of the future period, there are large changes in these relationships that may exhibit large interannual variability. The utilization of the historical track density and track intensity in a multivariable regression did not improve the precipitation predictions.

The underestimate of precipitation is quite different to the results of Chang et al. (2015), in that they found a one-to-one relationship between predicted and CMIP5 projected precipitation. One factor that could determine these differences could be the metric used to determine the storm-track activity in the different studies. Unlike Chang et al. (2015), the Lagrangian feature identification and tracking used here would not include variations associated with fronts, which pp would. However, given that frontal activity in this region is projected to decrease in the RCP8.5 simulations (Catto et al. 2014), this does not explain the underestimation of the projected precipitation. The pp measure would also include variations in high pressure systems that would not necessarily be associated with rainfall and would give high values when storms are rapidly decaying in this region. It will be an interesting and necessary topic of future research to compare a number of storm-track

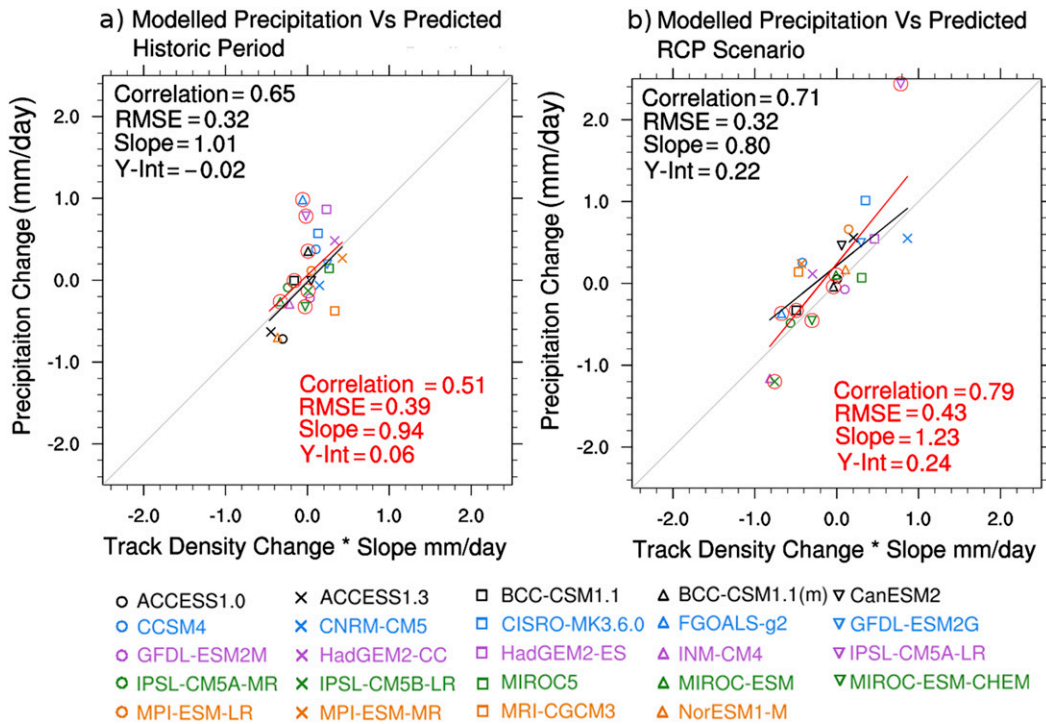


FIG. 9. The change in precipitation between (a) 1965–85 and 1985–2005 was “predicted” using the change in track density (cyclones per month per 5°-radius circle) between those time periods, which was multiplied by the regression coefficient between track density and Californian precipitation between 1965 and 1985, and the analysis was repeated for the time period (b) 2060–80 and 2080–2100. The correlation, RMSE, slope, and y intercept for all models are shown in red while the same statistics, slope excluding lower-resolution models with a grid box area greater than 6° are shown in black. Excluded models (surrounded by a red circle) are BCC\_CSM1.1, BCC\_CSM1.1(m), FGOALS-g2, IPSL-CM5A-LR, IPSL-CM5B-LR, MIROC-ESM, and MIROC-ESM-CHEM. Individual models are uniquely identified by a shape and color. The line  $y = x$  is shown in gray.

measures and how they relate to future changes in precipitation in this and other regions. Given the conclusions of a number of previous studies that suggest increases in precipitation intensity associated with extratropical cyclones in the future (Booth et al. 2013), the results of our study are perhaps more in line with what would be expected.

We found there is a greater variation between the CMIP5 models in the relationship between track intensity and precipitation compared with track density. This may reflect the varying representation of the shape of cyclones in terms of radius, depth, and intensity that is produced by each model (e.g., Catto et al. 2010). Two models may produce similar numbers of cyclones but differ in the distribution or intensity. Although not included in the present study this is another aspect for further investigation.

This study is complementary to that of Chang et al. (2015), showing that while the variability in the projected changes in the storm tracks is important for the variability in projected precipitation, the changing characteristics of cyclones will also have a large effect.

Our results are consistent with other studies that indicate that cyclone-relative precipitation is projected to increase in a moister world (Watterson 2006; Champion et al. 2011; Booth et al. 2013) and that rising humidity is a major driver of wetting in California in the winter season (Seager et al. 2014). Previous studies have also shown that increased moisture produces more intense cyclones (Booth et al. 2013; Pfahl et al. 2015), a result that we do not find with our methodology and that should be further investigated. Our results indicate that in the future, for the same number of cyclone tracks or track intensity more precipitation is received. Thus, knowing the changes in cyclone density and intensity is insufficient to predict changes in precipitation, an additional factor—likely moisture—must be considered.

**Acknowledgments.** This work was funded by the Australian Research Council (ARC) through a Discovery Early Career Research Award (DE140101305) and the Centre of Excellence for Climate Systems Science (CE110001028). ERA-Interim data are available online (<http://apps.ecmwf.int/datasets/>).

## REFERENCES

- Adler, R. F., and Coauthors, 2003: The Version-2 Global Precipitation Climatology Project (GPCP) monthly precipitation analysis (1979–present). *J. Hydrometeor.*, **4**, 1147–1167, [https://doi.org/10.1175/1525-7541\(2003\)004<1147:TVGCP>2.0.CO;2](https://doi.org/10.1175/1525-7541(2003)004<1147:TVGCP>2.0.CO;2).
- Booth, J. F., S. Wang, and L. Polvani, 2013: Midlatitude storms in a moister world: lessons from idealized baroclinic life cycle experiments. *Climate Dyn.*, **41**, 787–802, <https://doi.org/10.1007/s00382-012-1472-3>.
- Catto, J. L., L. C. Shaffrey, and K. I. Hodges, 2010: Can climate models capture the structure of extratropical cyclones? *J. Climate*, **23**, 1621–1635, <https://doi.org/10.1175/2009JCLI3318.1>.
- , —, and —, 2011: Northern Hemisphere extratropical cyclones in a warming climate in the HiGEM high-resolution climate model. *J. Climate*, **24**, 5336–5352, <https://doi.org/10.1175/2011JCLI4181.1>.
- , N. Nicholls, C. Jakob, and K. L. Shelton, 2014: Atmospheric fronts in current and future climates. *Geophys. Res. Lett.*, **41**, 7642–7650, <https://doi.org/10.1002/2014GL061943>.
- Cayan, D. R., and J. O. Roads, 1984: Local relationships between United States West Coast precipitation and monthly mean circulation parameters. *Mon. Wea. Rev.*, **112**, 1276–1282, [https://doi.org/10.1175/1520-0493\(1984\)112<1276:LRBUSW>2.0.CO;2](https://doi.org/10.1175/1520-0493(1984)112<1276:LRBUSW>2.0.CO;2).
- Champion, A. J., K. I. Hodges, L. O. Bengtsson, N. S. Keenlyside, and M. Esch, 2011: Impact of increasing resolution and a warmer climate on extreme weather from Northern Hemisphere extratropical cyclones. *Tellus*, **63A**, 893–906, <https://doi.org/10.1111/j.1600-0870.2011.00538.x>.
- Chang, E. K. M., 2013: CMIP5 projection of significant reduction in extratropical cyclone activity over North America. *J. Climate*, **26**, 9903–9922, <https://doi.org/10.1175/JCLI-D-13-0209.1>.
- , 2014: Impacts of background field removal on CMIP5 projected changes in Pacific winter cyclone activity. *J. Geophys. Res. Atmos.*, **119**, 4626–4639, <https://doi.org/10.1002/2013JD020746>.
- , Y. Guo, and X. Xia, 2012: CMIP5 multimodel ensemble projection of storm track change under global warming. *J. Geophys. Res.*, **117**, D23118, <https://doi.org/10.1029/2012JD018578>.
- , C. Zheng, P. Lanigan, A. M. Yau, and J. D. Neelin, 2015: Significant modulation of variability and projected change in California winter precipitation by extratropical cyclone activity. *Geophys. Res. Lett.*, **42**, 5983–5991, <https://doi.org/10.1002/2015GL064424>.
- Choi, J., J. Lu, S.-W. Son, D. M. Frierson, and J.-H. Yoon, 2016: Uncertainty in future projections of the North Pacific subtropical high and its implication for California winter precipitation change. *J. Geophys. Res. Atmos.*, **121**, 795–806, <https://doi.org/10.1002/2015JD023858>.
- Dee, D., and Coauthors, 2011: The ERA-Interim reanalysis: Configuration and performance of the data assimilation system. *Quart. J. Roy. Meteor. Soc.*, **137**, 553–597, <https://doi.org/10.1002/qj.828>.
- Gao, Y., L. R. Leung, J. Lu, Y. Liu, M. Huang, and Y. Qian, 2014: Robust spring drying in the southwestern US and seasonal migration of wet/dry patterns in a warmer climate. *Geophys. Res. Lett.*, **41**, 1745–1751, <https://doi.org/10.1002/2014GL059562>.
- Griffin, D., and K. J. Anchukaitis, 2014: How unusual is the 2012–2014 California drought? *Geophys. Res. Lett.*, **41**, 9017–9023, <https://doi.org/10.1002/2014GL062433>.
- Hodges, K., 1994: A general method for tracking analysis and its application to meteorological data. *Mon. Wea. Rev.*, **122**, 2573–2586, [https://doi.org/10.1175/1520-0493\(1994\)122<2573:AGMFTA>2.0.CO;2](https://doi.org/10.1175/1520-0493(1994)122<2573:AGMFTA>2.0.CO;2).
- , 1995: Feature tracking on the unit sphere. *Mon. Wea. Rev.*, **123**, 3458–3465, [https://doi.org/10.1175/1520-0493\(1995\)123<3458:FTOTUS>2.0.CO;2](https://doi.org/10.1175/1520-0493(1995)123<3458:FTOTUS>2.0.CO;2).
- Howitt, R., J. Medellín-Azuara, D. MacEwan, J. R. Lund, and D. Sumner, 2014: Economic analysis of the 2014 drought for California agriculture. University of California, Davis, Center for Watershed Sciences Rep., 27 pp., [https://watershed.ucdavis.edu/files/content/news/Economic\\_Impact\\_of\\_the\\_2014\\_California\\_Water\\_Drought.pdf](https://watershed.ucdavis.edu/files/content/news/Economic_Impact_of_the_2014_California_Water_Drought.pdf).
- , D. MacEwan, J. Medellín-Azuara, J. R. Lund, and D. Sumner, 2015: Economic analysis of the 2015 drought for California agriculture. University of California, Davis, Center for Watershed Sciences Rep., 31 pp., [https://watershed.ucdavis.edu/files/biblio/Final\\_Drought%20Report\\_08182015\\_Full\\_Report\\_WithAppendices.pdf](https://watershed.ucdavis.edu/files/biblio/Final_Drought%20Report_08182015_Full_Report_WithAppendices.pdf).
- Kalnay, E., and Coauthors, 1996: The NCEP/NCAR 40-Year Reanalysis Project. *Bull. Amer. Meteor. Soc.*, **77**, 437–471, [https://doi.org/10.1175/1520-0477\(1996\)077<0437:TNYRP>2.0.CO;2](https://doi.org/10.1175/1520-0477(1996)077<0437:TNYRP>2.0.CO;2).
- Lehmann, J., D. Coumou, K. Frieler, A. V. Eliseev, and A. Levermann, 2014: Future changes in extratropical storm tracks and baroclinicity under climate change. *Environ. Res. Lett.*, **9**, 084002, <https://doi.org/10.1088/1748-9326/9/8/084002>.
- Maloney, E. D., and Coauthors, 2014: North American climate in CMIP5 experiments: Part III: Assessment of twenty-first-century projections. *J. Climate*, **27**, 2230–2270, <https://doi.org/10.1175/JCLI-D-13-00273.1>.
- Medellín-Azuara, J., and Coauthors, 2016: Economic analysis of the 2016 California drought on agriculture. University of California, Davis, Center for Watershed Sciences Rep., 20 pp., [https://watershed.ucdavis.edu/files/DroughtReport\\_20160812.pdf](https://watershed.ucdavis.edu/files/DroughtReport_20160812.pdf).
- Mizuta, R., 2012: Intensification of extratropical cyclones associated with the polar jet change in the CMIP5 global warming projections. *Geophys. Res. Lett.*, **39**, L19707, <https://doi.org/10.1029/2012GL053032>.
- Neelin, J. D., B. Langenbrunner, J. E. Meyerson, A. Hall, and N. Berg, 2013: California winter precipitation change under global warming in the Coupled Model Intercomparison Project phase 5 ensemble. *J. Climate*, **26**, 6238–6256, <https://doi.org/10.1175/JCLI-D-12-00514.1>.
- Pfahl, S., and M. Sprenger, 2016: On the relationship between extratropical cyclone precipitation and intensity. *Geophys. Res. Lett.*, **43**, 1752–1758, <https://doi.org/10.1002/2016GL068018>.
- , P. O’Gorman, and M. S. Singh, 2015: Extratropical cyclones in idealized simulations of changed climates. *J. Climate*, **28**, 9373–9392, <https://doi.org/10.1175/JCLI-D-14-00816.1>.
- Scheff, J., and D. Frierson, 2012: Twenty-first-century multimodel subtropical precipitation declines are mostly midlatitude shifts. *J. Climate*, **25**, 4330–4347, <https://doi.org/10.1175/JCLI-D-11-00393.1>.
- Seager, R., and Coauthors, 2014: Dynamical and thermodynamical causes of large-scale changes in the hydrological cycle over North America in response to global warming. *J. Climate*, **27**, 7921–7948, <https://doi.org/10.1175/JCLI-D-14-00153.1>.
- , M. Hoerling, S. Schubert, H. Wang, B. Lyon, A. Kumar, J. Nakamura, and N. Henderson, 2015: Causes of the 2011–14 California drought. *J. Climate*, **28**, 6997–7024, <https://doi.org/10.1175/JCLI-D-14-00860.1>.
- Swain, D. L., M. Tsiang, M. Haugen, D. Singh, A. Charland, B. Rajaratnam, and N. S. Diffenbaugh, 2014: The extraordinary California drought of 2013/2014: Character, context, and the role of climate change [in “Explaining Extreme Events of

- 2013 from a Climate Perspective”]. *Bull. Amer. Meteor. Soc.*, **95** (9), S3–S7.
- Tamarin-Bordsky, T., and Y. Kaspi, 2017: Enhanced poleward propagation of storms under climate change. *Nat. Geosci.*, **10**, 908–913, <https://doi.org/10.1038/s41561-017-0001-8>.
- Taylor, K. E., R. J. Stouffer, and G. A. Meehl, 2012: An overview of CMIP5 and the experiment design. *Bull. Amer. Meteor. Soc.*, **93**, 485–498, <https://doi.org/10.1175/BAMS-D-11-00094.1>.
- Vose, R. S., and Coauthors, 2014: Improved historical temperature and precipitation time series for us climate divisions. *J. Appl. Meteor. Climatol.*, **53**, 1232–1251, <https://doi.org/10.1175/JAMC-D-13-0248.1>.
- Wang, H., and S. Schubert, 2014: Causes of the extreme dry conditions over California during early 2013 [in “Explaining Extreme Events of 2013 from a Climate Perspective”]. *Bull. Amer. Meteor. Soc.*, **95** (9), S7–S11.
- Watterson, I. G., 2006: The intensity of precipitation during extratropical cyclones in global warming simulations: A link to cyclone intensity? *Tellus*, **58A**, 82–97, <https://doi.org/10.1111/j.1600-0870.2006.00147.x>.